



HAL
open science

Revealing systematic errors in hole drilling measurements through a calibration bench: the case of zero-depth data

Marco Beghini, Tommaso Grossi, Ciro Santus, Emilio Valentini

► To cite this version:

Marco Beghini, Tommaso Grossi, Ciro Santus, Emilio Valentini. Revealing systematic errors in hole drilling measurements through a calibration bench: the case of zero-depth data. *Journal of Theoretical, Computational and Applied Mechanics*, 2023, 10.46298/jtcam.10080 . hal-03721795v2

HAL Id: hal-03721795

<https://hal.science/hal-03721795v2>

Submitted on 31 Oct 2023

HAL is a multi-disciplinary open access archive for the deposit and dissemination of scientific research documents, whether they are published or not. The documents may come from teaching and research institutions in France or abroad, or from public or private research centers.

L'archive ouverte pluridisciplinaire **HAL**, est destinée au dépôt et à la diffusion de documents scientifiques de niveau recherche, publiés ou non, émanant des établissements d'enseignement et de recherche français ou étrangers, des laboratoires publics ou privés.



Distributed under a Creative Commons Attribution 4.0 International License

Identifiers

DOI 10.46298/jtcam.10080

HAL hal-03721795v2

History

Received Sep 26, 2022

Accepted May 4, 2023

Published Jun 6, 2023

Associate Editor

Laszlo S. TOTH

Reviewers

Michael PRIME

Anonymous

Open Review

OAI hal-04166396

Licence

CC BY 4.0

©The Authors

Revealing systematic errors in hole drilling measurements through a calibration bench: the case of zero-depth data

✉ Marco BEGHINI¹, ✉ Tommaso GROSSI¹, ✉ Ciro SANTUS¹, and Emilio VALENTINI²

¹ Department of Civil and Industrial Engineering, University of Pisa, Pisa, Italy

² SINT Technology Srl, Florence, Italy

An accurate estimation of the measurement error in the hole drilling method is needed to choose an appropriate level of regularization and to perform a sensitivity analysis on the stress results. The latest release of ASTM E837 standard for the hole drilling method includes a procedure aimed at estimating the standard deviation of the random error component on strain measurements, proposed by Schajer. Nevertheless, strain measurements are also affected to some extent by systematic errors which are not included in the estimation and need to be compensated. For example, an error in the rosette gage factor or in the identification of the zero-depth datum systematically affects all strain measurements in a strongly correlated fashion. This paper describes a calibration bench, designed to superimpose a reference bending stress distribution on a given specimen while simultaneously performing a hole drilling measurement. Since the reference solution is known a priori and shares the measurement instrumentation, the hole geometry and the stepping process with the actual residual stress distribution, the bench provides the user with a direct validation of the obtained accuracy. In addition, strategies aimed at compensating systematic errors can be tested on the reference solution and then applied on the residual stress evaluation. The imperfect hole geometry and drilling alignment are proven to cause a significant underestimation of stresses near the surface, as they lead to an incorrect identification of the zero-depth datum. It is shown that this effect can be corrected through the proposed calibration bench.

Keywords: residual stress, hole drilling, bench, systematic errors

1 Introduction

The hole drilling method (HDM) (Beaney 1976; Schajer 1981; Schajer 1988a; Schajer 1988b) is a widely used technique for evaluating residual stresses, due to its relatively low cost and its in-field applicability. Commercially available devices such as MTS3000-Restan by SINT Technology provide the industrial user with suitable systems to perform the HDM ASTM procedure E837 (American Society for Testing and Materials 2020). Its physical principle consists in the fact that drilling a hole in a stressed specimen produces strain relaxations in the material surrounding the hole. By measuring strains at increasing hole depths, the residual stress distributions along the depth, in the area where the hole was drilled, can be obtained. Technical and mathematical details of the procedure can be found in (Schajer and Whitehead 2013, Ch. 2).

Under the assumption of homogeneous isotropic linear elastic material, small strains, and plane stress state (due to the relatively low hole depth), the residual stress solutions can be obtained from a linear system of the form

$$As = e \quad (1)$$

where e is a vector collecting the measured strains ϵ_i at various hole depths, s , a vector containing the identified residual stresses, and A , a calibration matrix—obtained through FEM analyses—which linearly connects the two vectors. A three strain gauges rosette is needed to identify a

general plane stress state, and Schajer (1988a) showed that the three readings can be linearly combined to obtain three decoupled equations like Equation (1). With the Integral Method (IM) (Schajer 1988a; Schajer 1988b), stress distributions are assumed to be piecewise constant functions, whose discrete values are stored in s . Other general mathematical forms can be assumed to obtain a linear system like Equation (1); for example, see the Influence Functions Method (IFM) (Beghini et al. 2010a; Beghini et al. 2010b) or the Power Series Method (Schajer 1981).

The HDM presents two mathematical peculiarities: 1) it gets substantially ill-conditioned (Beghini et al. 2023b) when the hole steps are reduced in size to obtain residual stresses with a finer spatial resolution; 2) relaxed strains at a given hole depth depend only on stress values at lower depths. The former implies that strain errors need to be characterized and properly mitigated. The latter means that when Equation (1) is constructed through the IM, matrix A is lower-triangular, thus the identified stress values near the surface are determined by the first few values of measured strains.

The latest release of ASTM E837 standard includes a procedure to estimate random errors (namely, errors which affect every strain measurement randomly, such as electrical noise) and to filter them through Tikhonov regularization (Schajer 2007). As observed in (Schajer and Altus 1996) and (Olson et al. 2021), strains are also affected by systematic errors which are not included in the estimation since they affect all measurements in a strongly correlated fashion, such as errors in the rosette gage factors or in the identification of the zero-depth point.

In Figure 1, a calibration bench is presented, aimed at detecting and correcting these kinds of measurement biases by checking that the identified residual stresses match a known stress distribution. It has been designed and manufactured during a research collaboration between

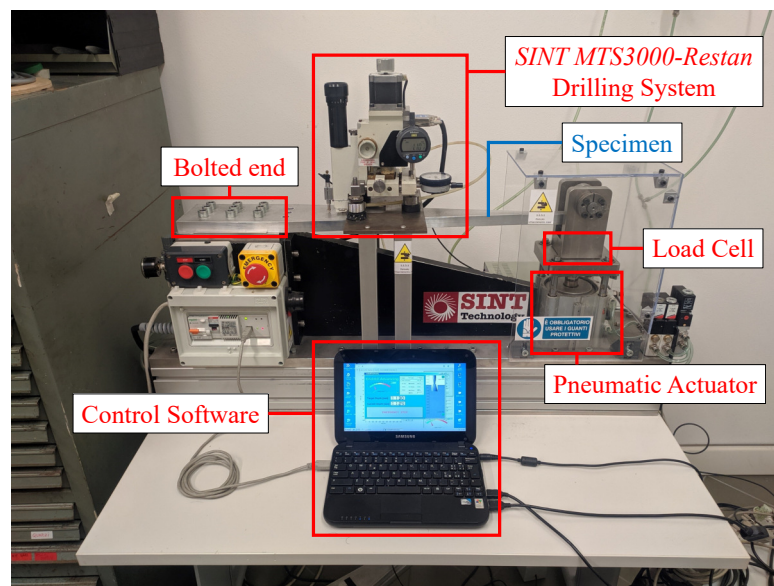


Figure 1 Description of the calibration bench.

SINT Technology and the Department of Civil and Industrial Engineering at University of Pisa, as a development of the one described in (Valentini et al. 2011)

2 Calibration bench

The bench is made up by a system which can impose a ≈ 40 mm vertical deflection by means of a pneumatic cylinder to the unsupported end of a 7075-T651 cantilever beam. The generated load is measured through a donut load cell, placed between the piston rod and the contact point with the specimen. The HDM procedure is carried out on the latter; its technical drawing is reported in Figure 2. It has a tapered central section, and the load application point is determined so as to produce constant bending stresses on the upper and lower faces of the tapered region. The specimen material could be changed, as long as its thickness is adjusted in order to generate the desired values of bending stresses and piston load.

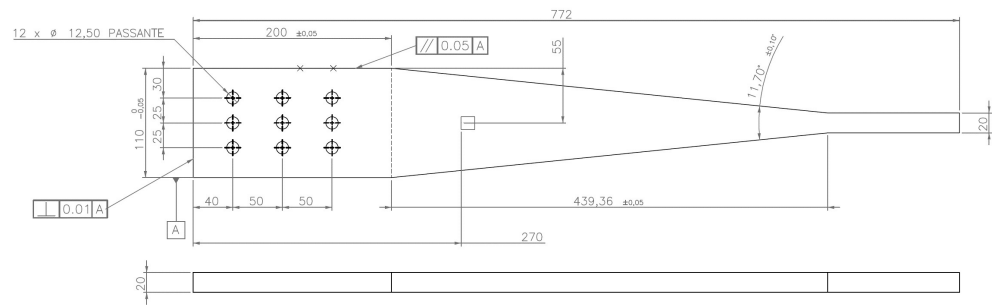


Figure 2 Technical drawing of the specimen, realized in 7075-T651 aluminum. A conventional strain rosette position is reported, but it can be placed reasonably anywhere in the tapered region.

The HDM procedure is carried out with the MTS3000-Restan hole drilling equipment, produced by SINT Technology. Details of the system and of the test procedure are available in (Valentini et al. 2007; Beghini et al. 2022; Beghini et al. 2023a).

Through the pneumatic actuator, the external load can be applied and removed without disassembling any part of the system. This allows the user to measure both relaxed strains corresponding to bending stresses and relaxed strains corresponding to actual residual stresses in the specimen. Both stress distributions share their experimental setup, so they also share most of the factors which may introduce biases in the identification process. If biases are absent and random errors are properly filtered, the identified bending stress shall correspond to the applied distribution. Alternatively, the bench may be used to validate strategies aimed at correcting those biases.

In this work, two examples are provided. The first shows how the bench can be used to check the strain gauge setup and the material elastic constants; the second shows how errors on the identification of the zero-depth datum can be corrected.

2.1 Strain gauge setup and material elastic constants

First, the reference system is defined as in Figure 3. The x axis is aligned with the specimen

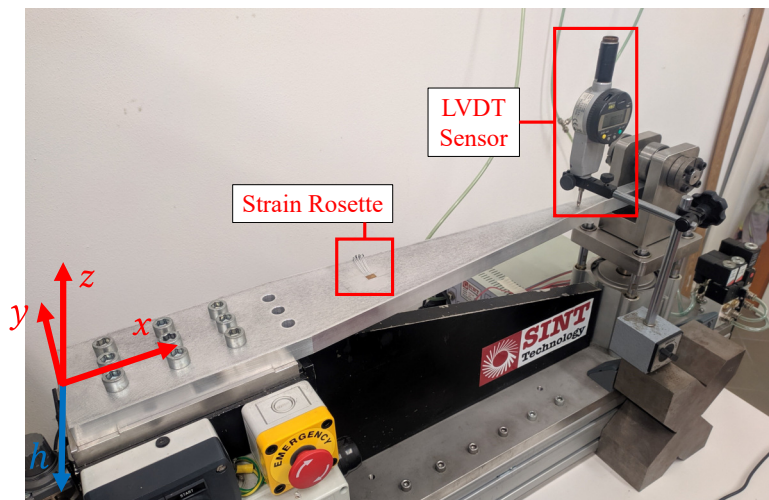


Figure 3 Specimen reference system and strain rosette calibration procedure. The external load was applied and the specimen deflection in z -direction was measured at nine points on the specimen x -axis with a LVDT transducer. Note that hole steps are drilled towards negative values of z ; nevertheless, the hole depth h is defined as a positive quantity.

longitudinal axis, the z axis points outwards from the upper face of the specimen, and the y axis follows consequently. A FEM model of the specimen was built in ANSYS (see Figure 4) and was correlated with the physical system. To do this, an LVDT transducer (resolution: ± 0.001 mm, uncertainty: ± 0.005 mm) was used to measure the vertical deflection at nine points on the tapered region between $x = 250$ mm and $x = 650$ mm, then values were compared with FEM results.

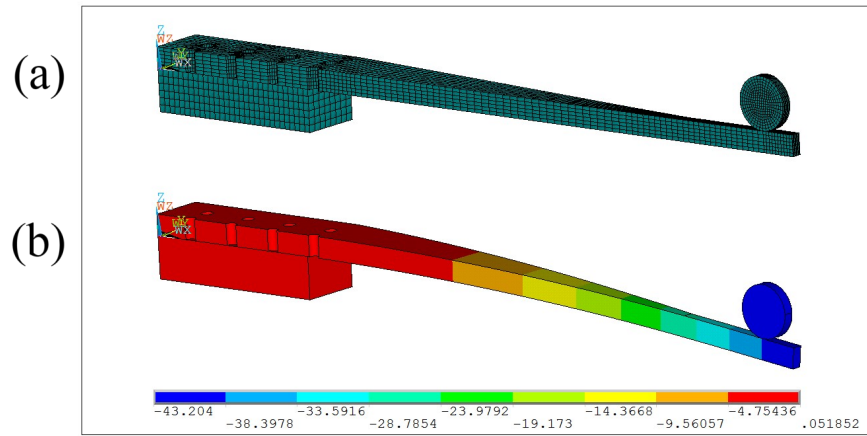


Figure 4 (a) FEM model of the specimen, built with second-order solid hexahedral elements. An end-displacement is applied to the bearing which transfers the piston load to the specimen. Symmetry about plane xz is exploited to reduce the model computational complexity. Contact elements are used to model the bolted constraints and the interface between the bearing and the specimen end. (b) Deflections in z -direction from the FEM model.

According to Euler-Bernoulli beam theory, the tapered region shows a uniform curvature when deflected. This hypothesis was verified by fitting deflection measurements with a quadratic formula: both experimental and FEM deflections were fitted with a maximum residual of less than 0.02 mm, which confirms the assumption. It was also checked that the effects of shear deformation on the curvature of the tapered region were negligible.

As the maximum displacement is imposed, the deflections are independent of the material elastic constants, which can be set freely in the FEM model. Two factors prevent the two deflections from matching: the actual compliance of the bolted end and the actual displacement imposed by the piston, which is not precisely known due to free-plays and compliances. The first can only give rise to a rigid body motion which does not affect the curvature (hence the strains) in the tapered region, so the experimental and modeled curvature must match. Therefore, the end-displacement applied to the FEM model were tuned until the experimental and modeled curvature were the same. Results are shown in Figure 5.

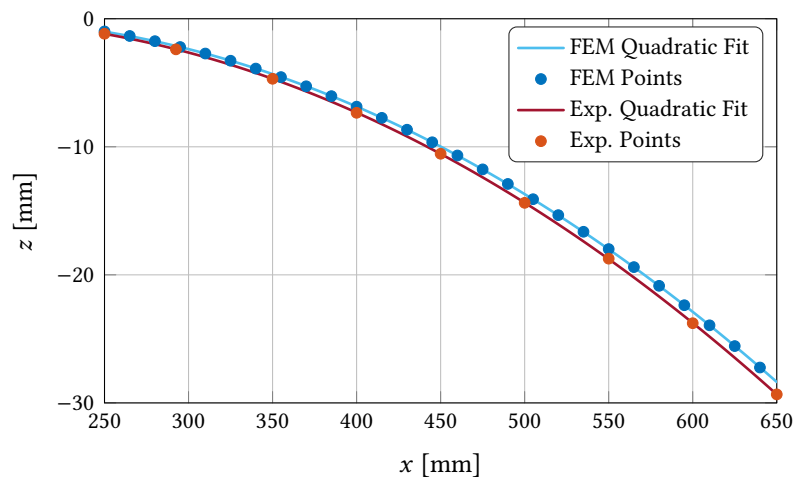


Figure 5 Specimen deflections in z -direction, along the tapered zone: comparison between experimental measurements (red points) and FEM outputs (blue points) after the calibration procedure which yielded an end-deflection of 38.76 mm. The two datasets were fitted with a quadratic expression, and the FEM applied end-displacement was adjusted until the two expressions yielded the same curvature. A linear difference in the deflections still remains (generated by a different constraint stiffness), but it does not affect strains in the tapered region. The actual constraint stiffness is slightly lower than its FEM prediction.

This process does not require elastic constants nor the applied load to be known, hence it does not depend on errors on those quantities. A sensitivity analysis shows that the experimental

curvature is known up to an accuracy of 0.1 %, which is likely to be at least as accurate as FEM results. The strain rosette shall measure a positive principal strain that matches the ϵ_{xx} resulting from the FEM model within tolerance on gauge factor values, otherwise the strain gauge setup should be checked. The orientation of the measured principal strains with respect to the specimen longitudinal axis can also be checked. The rosette gage factors may be isotropically scaled to adjust the principal measured strain to its corresponding FEM value. The Poisson ratio ν of the material can be identified from the ratio of the two measured principal strains, up to an accuracy which depends on the variability of gauge factors among strain grids.

The applied load is measured with the load cell, and it is equal to 2357 N in this setup; the stress σ_{xx} in correspondence of the strain gauge can be evaluated from beam theory (164.4 MPa). Therefore, the (secant) Young's modulus of the material can be identified as the ratio between σ_{xx} and ϵ_{xx} . Its accuracy mainly depends on the uncertainties on load cell measurements, whose relative magnitude may be conservatively estimated in the order of a percentage point.

An HBM RY61K strain rosette was glued to the specimen at $x = 292.5$ mm, aligned with the specimen reference system as shown in Figure 6. Then, this procedure was applied to check the

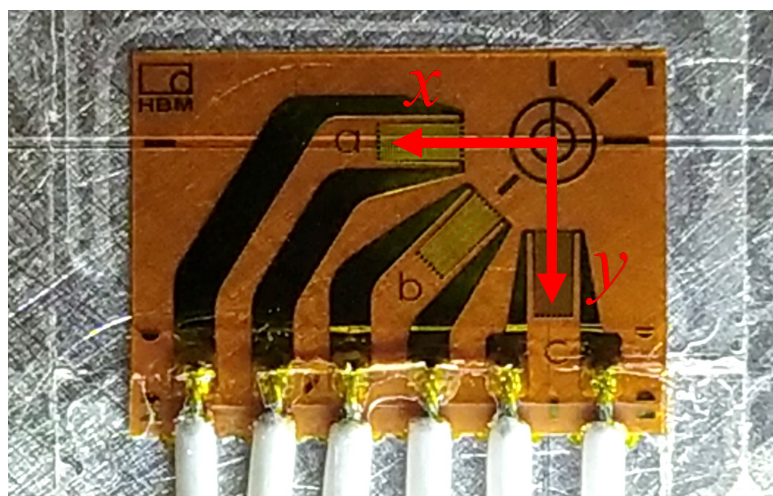


Figure 6 Strain rosette (HBM RY61K) applied on the upper face of the specimen at $x = 292.5$ mm, aligned with the specimen reference system. Grid naming (a, b and c) is printed on the rosette itself.

rosette gauge factors and the elastic constants of the material. The rosette measured a maximum principal strain of $2362 \mu\epsilon$, while the FEM analysis showed a $\epsilon_{xx} = 2347 \mu\epsilon$ at that point. The difference is less than 1 %, hence compatible with the gauge factor tolerance specified by the producer; it was compensated by scaling strain measurements. Young's modulus of the material was identified at 70 GPa. Results are summarized in Table 1.

	Experimental	FEM
Deflections quadratic fit (mm)	$-1.176 \cdot 10^{-4}x^2 + 3.55 \cdot 10^{-2}x - 2.69$	$-1.176 \cdot 10^{-4}x^2 + 3.75 \cdot 10^{-2}x - 3.02$
ϵ_{xx} at $x = 292.5$ mm	$2362 \mu\epsilon$	$2347 \mu\epsilon$
σ_{xx} at $x = 292.5$ mm		164.4 MPa
Identified elastic constants		$E = 70.0$ GPa, $\nu = 0.31$
Strain rosette misalignment		0.25°

Table 1 Results of the correlation between experimental results and the FEM model. The principal strain measured by the strain rosette differs from the FEM strain by less than 1%, which is compatible with the gage factor tolerance. The elastic constants are coherent with a 7075-T651 aluminum and were used in the subsequent HDM procedure.

2.2 Zero depth-offset errors

An HDM procedure is carried out on the applied strain rosette. Using a 1.6 mm cutting tool, a maximum depth of $h = 1.2$ mm was reached through 120 increments of 0.01 mm (a positive depth

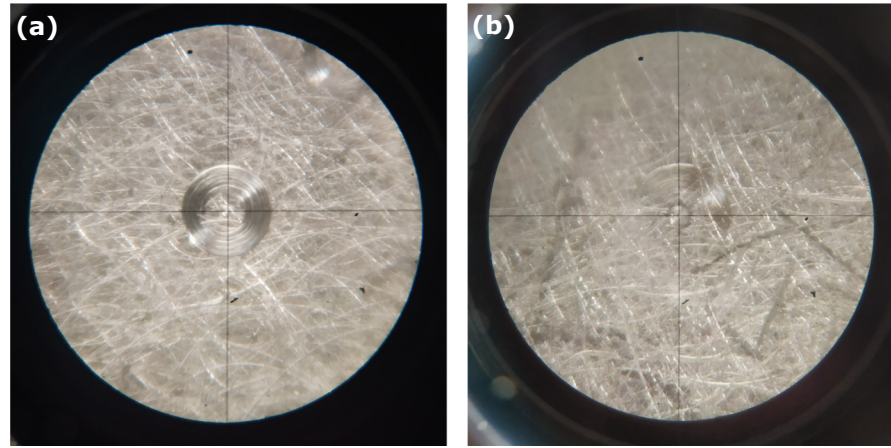


Figure 7 Examples of situations that generate errors in the reconstruction of residual stresses near the zero-depth point. Images were taken after a 10 μm drilling step from the identified zero-depth point (through electrical contact). (a) Non-planarity of the drilling tool yields a non-flat hole bottom surface. (b) Non-perpendicularity of the drilling axis with respect to the specimen surface yields a non-axisymmetric hole.

h is measured oppositely to the z direction, recall Figure 3). The hole step at depth h is performed without the external load applied, so that the relaxed strains measured by the i -th grid $\epsilon_i^{RS}(h)$ correspond to the actual residual stress distribution. Then, the deflection is produced through the piston, and the new strains $\epsilon_i^F(h)$ are recorded. The relaxed strains $\epsilon_i^{Be}(h)$ corresponding to the applied bending stresses can be evaluated as follows:

$$\epsilon_i^{Be}(h) = (\epsilon_i^F(h) - \epsilon_i^{RS}(0)) - \epsilon_i^{RS}(h). \tag{2}$$

Details of the procedure are available in (Valentini et al. 2011). In this work, only strains $\epsilon_i^{Be}(h)$ were considered and are plotted in Figure 8, as the actual residual stress distribution in the specimen was not analyzed.

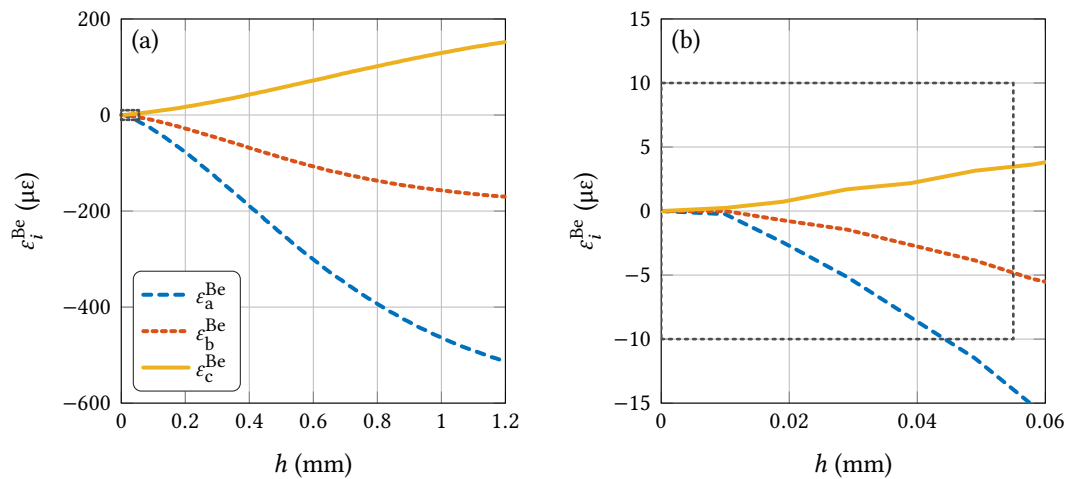


Figure 8 (a) Bending relaxed strains measured by the three gauges (a, b and c) on the rosette. A dashed grey rectangle highlights a region near the zero-depth point. (b) Zoom on the zero-depth point. A significant jump in the first derivatives of the three curves near the first acquired point ($h = 0.01$ mm) is qualitatively evident.

The zero-depth point was identified through electric contact between the drilling tool and the metallic specimen surface. By choosing a stress resolution of 0.02 mm, stresses corresponding to $\epsilon_i^{Be}(h)$ were evaluated through the IFM (assuming piecewise linear stress distributions) and processed with Tikhonov regularization and Morozov discrepancy principle, according to ASTM E837; they can be found in Figure 9(a). Note that ASTM E837 actually prescribes a maximum hole depth of 1 mm for the given strain rosette. The largest errors were found precisely in the zone

past 1 mm depth, where the sensitivity of the HDM starts failing, and near the zero-depth point, where other effects arise.

In Figure 7, the effects of imperfect drill surfaces and of tool misalignment are shown. Overall, they generate “delayed” strains (as qualitatively shown in Figure 8(b)) because a true cylindrical hole starts one or more steps after the first one. Although a precise modeling of a non-cylindrical hole falls outside the axisymmetric hole model used in the HDM, this effect can be seen as an error in the identification of the “true” zero-depth datum, as observed in (Valentini et al. 2011). For example, the effect of a 0.02 mm depth shift (compatible with Figure 7) of the strains is reported in Figure 9(b): the largest effect is precisely near the zero-depth point.

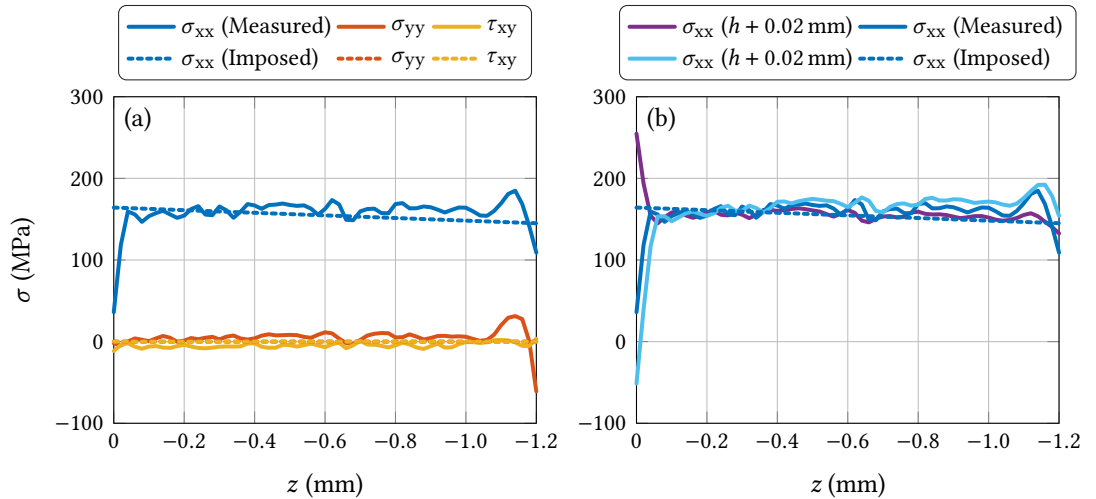


Figure 9 (a) Bending stress distributions corresponding to measured strains through the hole drilling method inverse problem. Calculation points are evenly spaced with a 0.02 mm step; strain inputs were processed through Tikhonov second-order regularization and Morozov discrepancy principle. (b) Effect of a translation in h of measured strains on the identified σ_{xx} . The most affected zone is near the zero-depth point, while the effect is less pronounced at higher depths.

Knowing this, the actual shift value may be manually tuned in order to reproduce the imposed bending stresses, as shown in Figure 10(a). However, this requires multiple time-consuming

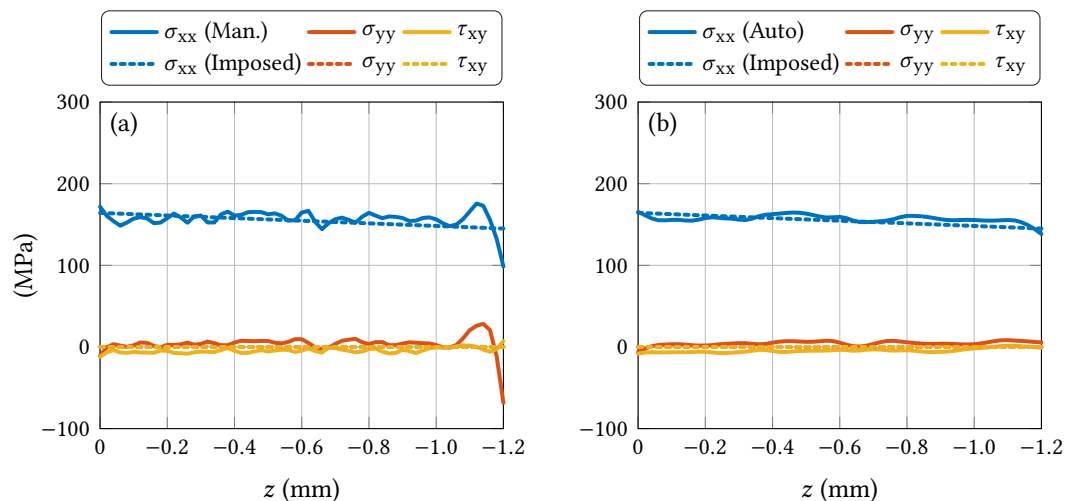


Figure 10 (a) Bending stress distributions corresponding to measured strains shifted by -0.012 mm, towards the zero-depth point. This specific shifting value has been chosen by manual tuning. (b) Bending stress distributions corresponding to measured strains whose depth shift has been automatically set to -0.0129 mm by the proposed procedure.

evaluations of matrix A in Equation (1), as it depends on the actual hole depths. Alternatively, another strategy is proposed here. At a first approximation, a small shift in depth Δh is equivalent to a strain variation of $\frac{d\epsilon}{dh}\Delta h$ at the same hole depths. Hence, while keeping matrix A constant

and modifying the strains only, Δh can be automatically chosen as the one which minimizes the norm of the stress second-order numerical derivative, to enforce smoothness and avoid the abrupt stress deviation near the surface. Results of this strategy are reported in Figure 10(b). It shall be observed that this procedure yields a significant improvement over uncompensated results, showing absolute errors of less than 10 MPa, even beyond the 1 mm depth limit prescribed by ASTM E837.

3 Conclusions


A calibration bench for the hole drilling method has been presented, together with some strategies aimed at validating the experimental setup and compensating potential biases in measurements. In particular:

- It allows a verification of the strain gauge readings which is independent from the uncertainties on the elastic constants of the material and on load measurements.
- It provides feedback on the correct application of the HDM procedure and a quantitative estimation of the errors on the identified residual stresses, as the calculated bending stress distribution can be compared with the applied one.
- It allows the validation of error compensation strategies. For example, it is shown that a zero-depth offset—which affects the identified stress distribution near the specimen surface—can be corrected after that the procedure has been carried out.
- Since the bench permits a simultaneous identification of residual and bending stresses, the compensations applied for the bending case (to improve correlation with imposed stresses) can be easily extended to actual residual stresses in the specimen, as they share most of the factors that may affect the hole-drilling method procedure, such as the hole geometry and eccentricity, the strain gauge setup, and a zero-depth offset. This approach increases the accuracy of the residual stress measurement and is investigated in separate works (Beghini et al. 2022; Beghini et al. 2023a; Beghini et al. 2023c). Therein, various surface treatments are analyzed, and hole-drilling measurements (before and after compensations) are compared with X-Ray diffraction measurements, which are not affected by the zero-depth issue.

References

- American Society for Testing and Materials (2020). *Test method for determining residual stresses by the hole-drilling strain-gage method*. ASTM Standard: ASTM E837-20. [DOI].
- Beaney, E. M. (1976). Accurate measurement of residual stress on any steel using the centre hole method. *Strain* 12(3):99–106. [DOI].
- Beghini, M., L. Bertini, and L. F. Mori (2010a). Evaluating non-uniform residual stress by the hole-drilling method with concentric and eccentric holes. Part I: Definition and validation of the influence functions. *Strain* 46(4):324–336. [DOI].
- Beghini, M., L. Bertini, and L. F. Mori (2010b). Evaluating non-uniform residual stress by the hole-drilling method with concentric and eccentric holes. Part II: Application of the influence functions to the inverse problem. *Strain* 46(4):337–346. [DOI].
- Beghini, M., T. Grossi, C. Santus, L. Seralessandri, and S. Gulisano (2023a). Residual stress measurements on a deep rolled aluminum specimen through X-ray diffraction and hole-drilling, validated on a calibration bench. *IOP Conference Series: Materials Science and Engineering* 1275(1):012036. [DOI], [OA].
- Beghini, M., T. Grossi, C. Santus, A. Torboli, A. Benincasa, and M. Bandini (2022). X-ray diffraction and hole-drilling residual stress measurements of shot peening treatments validated on a calibration bench. *14th International Conference on Shot Peening* (Milan, Italy, Sept. 4–7, 2022). [HAL].
- Beghini, M., T. Grossi, M. B. Prime, and C. Santus (2023b). Ill-posedness and the bias-variance trade-off in residual stress measurement inverse solutions. *Experimental Mechanics* 63(3):495–516. [DOI], [OA].
- Beghini, M., T. Grossi, and C. Santus (2023c). Validation of a strain gauge rosette setup on a cantilever specimen: Application to a calibration bench for residual stresses. *Materials Today*:

- Proceedings*. [DOI], [OA].
- Olson, M. D., A. T. DeWald, and M. R. Hill (2021). Precision of hole-drilling residual stress depth profile measurements and an updated uncertainty estimator. *Experimental Mechanics* 61(3):549–564. [DOI], [OA].
- Schajer, G. S. (1981). Application of finite element calculations to residual stress measurements. *Journal of Engineering Materials and Technology* 103(2):157–163. [DOI].
- Schajer, G. S. (1988a). Measurement of non-uniform residual stresses using the hole-drilling method. Part I. Stress calculation procedures. *Journal of Engineering Materials and Technology* 110(4):338–343. [DOI].
- Schajer, G. S. (1988b). Measurement of non-uniform residual stresses using the hole-drilling method. Part II. Practical application of the Integral Method. *Journal of Engineering Materials and Technology* 110(4):344–349. [DOI].
- Schajer, G. S. and E. Altus (1996). Stress calculation error analysis for incremental hole-drilling residual stress measurements. *Journal of Engineering Materials and Technology* 118(1):120–126. [DOI].
- Schajer, G. and P. Whitehead (2013). Hole drilling and ring coring. *Practical Residual Stress Measurement Methods*. Ed. by G. Schajer. John Wiley & Sons. Chap. 2, pp 29–64. [DOI].
- Schajer, G. S. (2007). Hole-drilling residual stress profiling with automated smoothing. *Journal of Engineering Materials and Technology* 129(3):440–445. [DOI].
- Valentini, E., M. Beghini, L. Bertini, C. Santus, and M. Benedetti (2011). Procedure to perform a validated incremental hole drilling measurement: Application to shot peening residual stresses: validated IHD measurement test rig. *Strain* 47:e605–e618. [DOI].
- Valentini, E., M. Benedetti, V. Fontanari, M. Beghini, L. Bertini, and C. Santus (2007). Fine increment hole-drilling method for residual stress measurement, proposal of a calibrating apparatus. *Experimental Analysis of Nano and Engineering Materials and Structures*. Springer, pp 945–946. [DOI].

Open Access This article is licensed under a Creative Commons Attribution 4.0 International License, which permits use, sharing, adaptation, distribution and reproduction in any medium or format, as long as you give appropriate credit to the original author(s) and the source, provide a link to the Creative Commons license, and indicate if changes were made. The images or other third party material in this article are included in the article's Creative Commons license, unless indicated otherwise in a credit line to the material. If material is not included in the article's Creative Commons license and your intended use is not permitted by statutory regulation or exceeds the permitted use, you will need to obtain permission directly from the authors—the copyright holder. To view a copy of this license, visit creativecommons.org/licenses/by/4.0. 

Authors' contributions MB: Conceptualization, Methodology, Investigation, Writing – review & editing, Supervision, Funding acquisition. TG: Conceptualization, Methodology, Software, Validation, Formal analysis, Investigation, Data curation, Writing – original draft. CS: Conceptualization, Methodology, Investigation, Writing – review & editing, Supervision, Funding acquisition. EV: Conceptualization, Methodology, Supervision, Funding acquisition.

Supplementary Material None.

Acknowledgements Alessio BENINCASA and Simone GULISANO of SINT Technology Srl are gratefully acknowledged for their contributions to the bench design.

Funding None.

Ethics approval and consent to participate Not applicable.

Consent for publication Not applicable.

Competing interests The authors declare that they have no competing interests.

Journal's Note JTCAM remains neutral with regard to the content of the publication and institutional affiliations.